

Single photon imaging spectrometers using superconducting tunnel junctions

L Frunzio, CM Wilson, K Segall, L Li, S Friedrich, MC Gaidis and DE Prober

Yale University, Applied Physics, P.O. Box 208284, New Haven, CT 06520-8284, USA

ABSTRACT: We are developing single photon 1-D and 2-D imaging spectrometers using superconducting tunnel junctions for astrophysical applications. They can operate in the energy range from X-ray to NIR. Our devices utilize a lateral trapping geometry. They have superconducting tunnel junctions on the sides of the absorber far apart from it. Energy information is obtained by the total collected charge. Position information is obtained from the fraction of the total charge collected by each junction. These devices perform intrinsic imaging with many more pixels than read out channels.

1. INTRODUCTION

Superconductive tunnel junctions (STJ) have been extensively studied in the development of single photon spectrometers in a large variety of configurations (Booth 1996). These detectors have been operated at energies ranging from the X-ray down to the Near Infrared (NIR) (Frank 1998, Lumb 1995, Verhoeve 1997). In the last years, they have been integrated in different devices which also perform imaging (Kraus 1989, Jochum 1993, Friedrich 1996, Rando 1998a). The general approach pursued to date is large format arrays of single pixel detectors up to about hundred (Rando 1998b).

We have developed STJ-based detectors with intrinsic 1-D imaging, meaning that the detectors have many more pixels than read out channels. We have done this employing lateral trapping and band gap engineering. In Fig. 1 is a schematic of the devices.

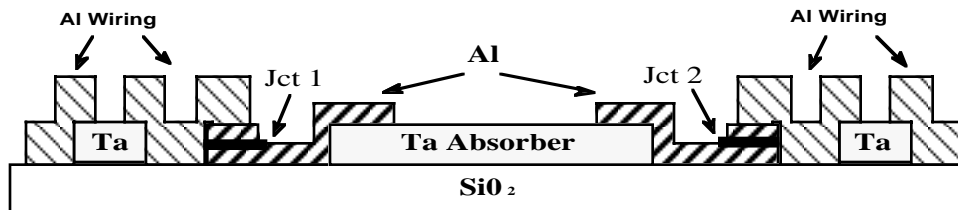


Figure 1. Schematic of a single photon 1-D imaging spectrometer using lateral trapping band gap engineering and backtunneling. Not shown is an insulating SiO layer between the junction and the wiring. In X-ray devices Ta plugs are not present.

2. OPERATING PRINCIPLE

Many physical processes are involved in the operation of these STJ-based detectors. First, an incident photon is absorbed in the central Ta film breaking Cooper pairs and creating quasiparticles. The quasiparticles relax down to the absorber gap energy and diffuse until they reach the Al. In the Al, they can scatter inelastically, losing energy until they reach the Al gap energy. Once the quasiparticles scatter below the gap of Ta by emission of phonons, they are “trapped” in the Al electrode. This trapping process also produces charge multiplication due to the fraction of emitted phonons with energy larger than twice the Al gap energy. Then, the quasiparticles tunnel and are read out as an excess subgap current. The current pulses are then integrated to obtain the charge collected from each junction.

The total collected charge is proportional to the ratio of the impinging photon energy and the effective energy required to excite a quasiparticle. The latter is proportional to the Ta absorber gap energy. The fraction of charge collected in each junction tells us the location of the absorption event. If the photon is absorbed in the center, then the charge divides equally. If the photon is absorbed at one edge of the absorber, then most of the charge is collected by the closest junction.

Another important process in our optical/UV detectors is backtunneling. Excited quasiparticles enter the Al base electrode from the Ta absorber and scatter down in energy. The higher energy gap of the Ta then confines the quasiparticles near the tunnel barrier. A Ta plug is added interrupting the Al wiring, confining the quasiparticles near the barrier in the counterelectrode. Quasiparticles can then circulate, tunneling and backtunneling. Because both tunneling and backtunneling transfer a charge in the forward direction, we measure an integrated charge many times greater than the number of quasiparticles. This effect gives the junctions charge gain, which is very important for the smaller signals in optical/UV devices.

The energy resolution is the sum in quadrature of many components taking into account creation statistics, the trapping process, the backtunneling, the incomplete cooling of the quasiparticles and the electronic noise. A full explanation of the noise mechanisms in these devices has been presented elsewhere (Segall 1999a)

In the limit of negligible loss in the absorber and complete quasiparticle trapping in the STJ base electrode, the number of pixel is proportional to the resolving power of the spectrometer (Wilson 1999) allowing an intrinsic 1-D imaging capability with only two read out channels.

3. EXPERIMENTAL CONDITIONS

All devices are fabricated at Yale in a high vacuum deposition system with in-situ ion beam cleaning. We start with a wet oxidized Si substrate. The Ta absorber and plugs are then dc magnetron sputtered at 750 °C. Next a Nb ground contact is sputtered. The Al trilayer is then evaporated in one vacuum cycle. An SiO insulating layer is evaporated and finally Al wiring is evaporated. An in-situ ion beam cleaning is performed before each metal deposition to ensure good metallic contact. All layers are patterned photolithographically using either wet etching or lift-off (Gaidis 1994).

Measurements are made in a two stage ³He dewar with a base temperature is 220 mK (Friedrich 1997a). To measure the photo-response of our junctions, we used a room temperature JFET current amplifier. We use an Amptek A250 amplifier with a 2SK146 input transistor. Extra circuitry is added that allows the A250/2SK146 to be dc coupled to the junctions. The amplifier thus provides an active voltage bias for the junction (Friedrich 1997b).

For X-ray measurements, we irradiate the sample with a ⁵⁵Fe source that emits two Mn lines at 5.89 keV (K_{α}) and 6.49 keV (K_{β}). In the optical/UV range, we illuminate the detectors using a small Hg lamp calibration source. A bandpass filter is used to select one photon energy at a time. We bring light into the dewar using an optical fiber, which is UV grade fused silica. The fiber is Al coated to enhance UV transmission up to energies of about 6 eV (200 nm). The filtered light passes through a fiber splitter that divides the light equally between two fibers. One of these fibers is fed into the dewar. The other fiber is fed into a photomultiplier tube which simultaneously measures the intensity.

4. RESULTS

We have made high quality Ta films with a residual resistance ratio of 17. The film are about 600 nm thick and are calculated to absorb about 28% of the incident energy at 6 keV. We have measured a quasiparticle loss time in the absorber of 450 μ s at 220 mK. This loss time can be compared to a time of \sim 10 μ s needed for a quasiparticle to diffuse across the absorber and be trapped in the Al junction electrode. We have made high quality Al films with a residual resistance ratio of 12 and a quasiparticle loss time of 57 μ s at 220 mK. This loss time can be compared to the \sim 2 μ s tunnel time in a typical junction.

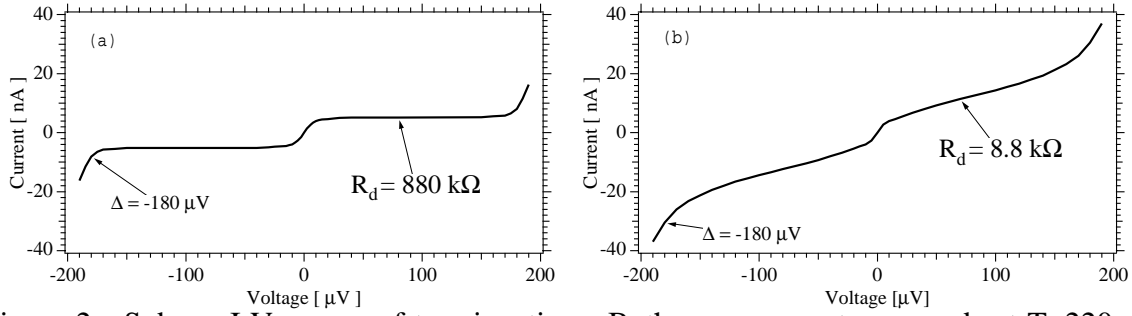


Figure 2. Subgap I-V curves of two junctions. Both measurements are made at $T=220$ mK. The junction parameters are: (a) Area= $400 \mu\text{m}^2$, $R_N=2.3 \Omega$; (b) Area= $100 \mu\text{m}^2$, $R_N=13.8 \Omega$.

We have also made high quality junctions. Two characteristics are important for low noise. First, junctions should have a low subgap current to minimize the shot noise. They should also have a large subgap resistance to minimize the contribution of the amplifier voltage noise. Fig. 2a shows the subgap I-V curve of a $400 \mu\text{m}^2$ junction with a normal state resistance $R_N=2.3 \Omega$. At 220 mK we measure a subgap current of 5 nA and a subgap resistance of 880 k Ω . Unfortunately, we have not been able to completely reproduce this quality in the imaging devices. Fig. 2b shows the subgap curve of a $100 \mu\text{m}^2$ junction from a different fabrication run. This junction has $R_N=13.8 \Omega$ and the subgap resistance is only 9 k Ω . We do not understand if this difference is a fabrication issue or an experimental setup problem.

We have detected single X-ray photons using many devices. A typical absorber has an active area of $160 \times 100 \mu\text{m}^2$. We use a junction area of either $560 \mu\text{m}^2$ or $1860 \mu\text{m}^2$. The latter have different wiring sizes and different trapping layer geometries (Friedrich 1997c). In some samples there are Ta plugs. More detailed results will be presented elsewhere. In any case, we have achieved an excellent energy resolution $\delta E_{\text{FWHM}}=26$ eV at 5.89 keV in a limited absorber length of about 34 μm . The best energy resolution obtained on a full active absorber length is $\delta E_{\text{FWHM}}=60$ eV at 5.89 keV. This energy resolution implies a spatial resolution of about 1.6 μm , thus providing 100 pixels with just two read out channels (Segall 1999b).



Figure 3. Photograph of the 1-D STJ-based imaging spectrometer tested in optical/UV range.

We have tested other detectors in the optical and ultraviolet region (Wilson 1999). Fig. 3 shows a typical device. The subgap curves of both its junctions look like the one in Fig. 2b. This device has a $100 \times 10 \mu\text{m}^2$ Ta absorber. Each Al trap overlaps the absorber by 5 μm . The presence of Ta plugs confines the quasiparticles near the barrier. We measure that the average number of times a quasiparticle tunnels is 23. The energy resolution, measured over the full absorber, is $\delta E_{\text{FWHM}}=1.0$ eV ($\delta\lambda=240$ nm) at $E=2.27$ eV ($\lambda=546$ nm) green line and $\delta E_{\text{FWHM}}=1.6$ eV ($\delta\lambda=83$ nm) at $E=4.89$ eV ($\lambda=253$ nm) UV line. For the UV if only a selected range of the absorber is chosen, we obtain $\delta E_{\text{FWHM}}=1.1$ eV ($\delta\lambda=57$ nm). We have measured the noise spectra of both junctions with no illumination and they are consistent with the measured resolution. However, the noise spectra contain excess noise that we cannot explain.

An energy resolving power of about 3 in the UV implies that the detector can resolve at least 4 spatial pixels at that energy. This particular detector has an active absorber area $90 \mu\text{m}$ long by $10 \mu\text{m}$ wide. So, the detector has 4 pixels with dimensions $22 \times 10 \mu\text{m}^2$. This is achieved with only two readout channels.

5. 2-D IMAGING

We are also developing single photon 2-D imaging spectrometers. For X-ray, we are studying the degrading of energy and spatial resolution of a 2-D absorber with traps at each side (Li 1999). We have begun fabricating these devices, one of those is shown in Fig. 4. Our Ta absorbers have very long quasiparticle loss time making feasible the realization of devices with 1 mm² absorber. Devices with large absorbers could resolve about 1000 of 20 x 20 μm² pixels with only four read out channels. For optical/UV, the limitations in the count rate resulting from this type of solution could be bypassed using array of strips, as shown in Fig. 4. In fact, this seems to be the best compromise between the needs of a large number of pixels with a simplified read out and the requirement on the count rate. Further improvements are feasible introducing an RF-SET based read out electronics (Schoelkopf 1998)

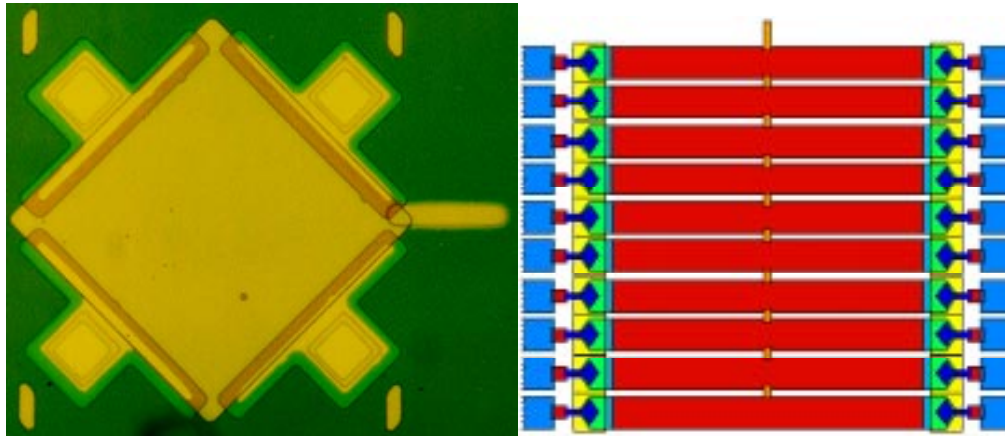


Figure 4. On the left: photograph of a 2-D X-ray imaging spectrometer fabricated at Yale before the wiring layer is deposited. On the right: diagram of a 2-D optical/UV imaging spectrometer using ten absorber strips.

6. CONCLUSIONS

We are developing and testing STJ-based single photon imaging spectrometers. Our devices use a lateral trapping and bandgap engineering. We have detected single X-ray, optical and UV photons with these first detectors.

REFERENCES

- Booth N E and Goldie D J 1996 *Supercond. Science and Technology* **9**, 493
- Frank M et al. 1998 *Rev. Sci. Instrum.* **69**, 25
- Friedrich S et al. 1996 *Nucl. Instrum. Meth. in Phys. Res.* **A370**, 44
- Friedrich S 1997a Ph.D Thesis, Yale University
- Friedrich S et al. 1997b *IEEE Trans. Appl. Supercond.* **7**, 3383
- Friedrich S et al. 1997c *Appl. Phys. Lett.* **71**, 3901
- Gaidis M C 1994 Ph.D Thesis, Yale University
- Jochum J et al. 1993 *Ann. Physik* **2**, 611
- Kraus H et al. 1989 *Phys. Lett.* **B231**, 195
- Li L et al. 1999 *Proc. LTD8* (in press)
- Lumb D H et al. 1995 *Proc. SPIE* **2518**, 258
- Rando N et al. 1998a *Proc. SPIE* **3435**
- Rando N et al. 1998b *Proc. SPIE* **3445-25**
- Schoelkopf R J et al. 1998 *Science* **280**, 1238
- Segall K et al. 1999a *Appl. Phys. Lett.* (submitted)
- Segall K et al. 1999b *IEEE Trans. Appl. Supercond.* (in press)
- Verhoeve P et al. 1997 *IEEE Trans. Appl. Supercond.* **7**, 3359
- Wilson C et al. 1999 *Proc. LTD8* (in press)